Biocompatibility of titanium implants modified by microarc oxidation and hydroxyapatite coating

Long-Hao Li, Hae-Won Kim, Su-Hee Lee, Young-Min Kong, Hyoun-Ee Kim
School of Materials Science and Engineering, Seoul National University, Seoul 151-742, Korea

Received 12 September 2004; revised 4 October 2004; accepted 4 October 2004
Published online 15 February 2005 in Wiley InterScience (www.interscience.wiley.com). DOI: 10.1002/jbm.a.30244

Abstract: A thin hydroxyapatite (HA) layer was coated on a microarc oxidized titanium (MAO-Ti) substrate by means of the sol–gel method. The microarc oxidation (anodizing) enhanced the biocompatibility of the Ti, and the bioactivity was improved further by the sol–gel HA coating on the anodized Ti. The HA sol was aged fully to obtain a stable and phase-pure HA, and the sol concentration was varied to alter the coating thickness. Through the sol–gel HA coating, the Ca and P concentrations in the coating layer increased significantly. However, the porous morphology and roughness of the MAO-Ti was altered very little by the sol–gel treatment. The proliferation and alkaline phosphatase (ALP) activity of the osteoblast-like cells on the MAO/HA sol–gel-treated Ti were significantly higher than those on the MAO-Ti without the HA sol–gel treatment. © 2005 Wiley Periodicals, Inc. J Biomed Mater Res 73A: 48–54, 2005

Key words: hydroxyapatite sol–gel coating; microarc oxidation (MAO); titanium, *in vitro* cell responses

INTRODUCTION

Pure titanium (Ti) and Ti alloys are widely used for dental and orthopedic implants, because of their high mechanical properties, chemical stability, and biocompatibility.[1] The biocompatibility of Ti is closely related to the properties of the surface oxide layer. Among the methods used to produce the oxide layer, the microarc oxidation (MAO) method has gained much interest, because both the roughness and chemical composition of the coating layer can be controlled by the MAO conditions.[2,3] When a positive voltage is applied to a Ti electrode placed in an electrolyte, an anodic oxidation (or anodizing) process occurs, and a porous TiO_2 layer is produced on the Ti surface. The TiO_2 layer generated by the MAO treatment was found to significantly improve the cellular activities of Ti *in vitro* and the bone-implant bonding properties *in vivo*.[4–8] These improvements were attributed to the increase in the surface roughness, as well as to the incorporation of Ca and P into the coating layer. The porous and rough morphology produced by the MAO process increased the cell attachment and mechanical interlocking of the tissue and implant. Moreover, the Ca and P sources, incorporated from the electrolyte into the coating layer, improved the osteoblast cell responses and further osseointegration. Usually, the morphological change and the Ca-P incorporation occur simultaneously with increasing MAO voltage. However, the incorporation of Ca-P, which was accomplished by controlling the electrolyte, has some limitations, because when increasing the incorporation of Ca-P by increasing the voltage, cracks were generated because of the increase in thickness of the coating layer. Ishizawa et al.[9] tried to form a CaP layer on the MAO treated Ti by means of a hydrothermal method. The existence of HA crystals on the MAO-treated Ti was reported to improve the bone bonding of Ti implants *in vivo*.

HA has frequently been used as a coating material on Ti implants to improve the cell responses and osteoconductivity[10–13] because it has chemical and crystallographic similarity to the inorganic component of hard tissues.[14,15] The HA coating layer formed by the sol–gel process was thin and smooth. Moreover, because this process is conducted under a liquid system, it is efficient for the coating of rough and complex-shaped materials.

In the present study, we formed a thin HA layer on the MAO-treated Ti by means of the sol–gel process. On the basis of our previous studies of sol–gel HA coatings,[11,12] we varied the sol concentration to adjust the Ca-P content and the morphology of the MAO-Ti system. The coating properties and *in vitro* osteoblast-like cell responses of the coatings were investigated.

Correspondence to: Hyoun-Ee Kim; e-mail: kimhe@snu.ac.kr
Contract grant sponsor: Korea Health 21 R&D Project, Ministry of Health & Welfare, Republic of Korea; contract grant number: 02-PJ3-PG6-EV11-0002

MATERIALS AND METHODS

Microarc oxidation (MAO)

Commercially available pure Ti (CP-Ti, grade 2; Ka-Hee Metal Industry Co., Seoul, Korea) in disk form (12 mm × 1 mm) was used as the substrate. The Ti disks were ground by using 400-grit SiC sandpaper and cleaned ultrasonically in acetone, ethanol and deionized water. First, the specimen was microarc oxidized (MAO) in an aqueous electrolyte at 270 V for 3 min, under a pulsed DC field. The frequency and duty [on-time/(on-time + off-time)] of the pulsed DC power were 660 Hz and 10%, respectively. The electrolyte contained 0.15*M* calcium acetate monohydrate (Samchun Pure Chemical Co., Ltd., Korea) and 0.02*M* calcium glycerophosphate (Kanto Chemical Co., Inc., Japan) as the internal source of Ca and P for the MAO treatment. The MAO was conducted in a water-cooled bath made of stainless steel, and a Ti plate (100 mm × 60 mm × 1 mm) was used as the counter electrode.

Sol–gel coating

Triethyl phosphite (Aldrich, USA) and calcium nitrate (Aldrich) were selected as the P and Ca sources, respectively.[16,17] Triethyl phosphite with a concentration of 1.8*M* was diluted in anhydrous ethanol, and deionized water was added for hydrolysis ([OH]/[P] = 12). The solution was sealed and stirred vigorously for 3 days to hydrolyze the triethyl phosphite fully. A stoichiometric amount of calcium nitrate (3*M*) was dissolved in anhydrous ethanol, and the p-containing solution was added dropwise to the Ca-containing solution. The mixed solution was stirred for 1 h and aged for 5 days at room temperature to obtain a fully aged HA sol. The aging time was determined from phase analyses to make a pure phase HA. The HA sols with different concentrations (1.5, 2, and 4*M*) were prepared similarly.

The MAO-treated Ti specimen (MAO-Ti) was spin-coated with the prepared HA sols at a spin rate of 3000 rpm for 40 s. The coated Ti was dried at 80°C for 2 h and then heat-treated at 550°C for 2 h at a heating rate of 2°C/min.

Characterization

The phase of the specimens were evaluated by X-ray diffraction (XRD; M18XHF-SRA, MacScience Co., Yokohama, Japan) with Cu Kα radiation at a scanning speed of 0.5° over a 2θ range of 25–40°. The microstructure of the specimens was observed with a scanning electron microscope (SEM; JSM-5600; JEOL, Tokyo, Japan). The composition of the surface layer was analyzed with an energy-dispersive spectroscope (EDS), which was connected to the scanning electron microscope. The surface roughness was measured by means of confocal laser scanning microscopy (OLS1200; Olympus Optical Co., Ltd., Tokyo, Japan). The average roughness (R_a) was used to characterize the roughness of the specimens, and the measured area was 50 μm × 50 μm. The average of at least five tests was used for each experimental measurement.

In vitro cell test

The biological performance of the coatings was evaluated by *in vitro* cell tests using a human osteosarcoma (HOS) cell line.[18] After subculturing for 3 days, the cell line was plated onto specimens at a cell density of 3×10^4 cells/mL for the proliferation and 1×10^4 cells/mL for the ALP test, and then cultured in a humidified incubator with 5% CO_2 at 37°C.

After culturing for 5 days, the cells were detached with 0.1% trypsin-EDTA, and the cell number was counted by using a hemocytometer (Superior Co., Germany). To assess the ALP activity, the cells were cultured for 5 and 10 days. After culturing, the cell layers were washed with Hank's balanced salt solution (HBSS) and detached by using trypsin-EDTA solution. After centrifugation at 1300 rpm for 5 min, the cell pellets were washed with PBS and resuspended by vortexing in 200 μL of 0.1% Triton X-100. The pellets were disrupted via a freezing-thawing process. After centrifugation, the cell lysates were assayed colorimetrically to measure their ALP activity using *p*-nitrophenyl phosphate as the substrate (kit no. 104; Sigma, USA). The reaction lasted for 60 min at 37°C and was then stopped by quenching on ice. The quantity of *p*-nitrophenol produced was measured at 410 nm by using a spectrophotometer (Shimadzu, Japan). The morphology of the proliferated cells was observed by a scanning electron microscope (SEM) after fixation with 2.5% glutaraldehyde, dehydration with graded ethanols (70, 90, and 100%), and critical point drying using CO_2. Each set of tests was performed on six replicate samples.

Statistical analysis

The experimental data were represented as means ± one standard deviations (SD) for $n = 6$. Statistical analysis was conducted via a one-way analysis of variance (ANOVA). The differences were considered to be significant at $p < 0.05$, $p < 0.01$, and $p < 0.001$.

RESULTS

Coating morphology

The surface morphologies of the HA sol–gel coating on the MAO treated Ti (MAO-Ti) substrate are shown in Figure 1(A–F). The pure Ti surface had some machining grooves [Fig. 1(A)]. After MAO treatment of the Ti at 270 V, a porous oxide layer was formed throughout the surface [Fig. 1(B)]. When the MAO-Ti was coated with an HA sol at a concentration of 1.5*M* and heat treated at 550°C, some of the large pores became slightly smaller. However, the surface appeared to maintain the initial morphology of the MAO-Ti to a high degree, due to the formation of an extremely thin HA layer [Fig. 1(C)]. As the sol concentration was increased (from 2 to 4*M*), some of the small

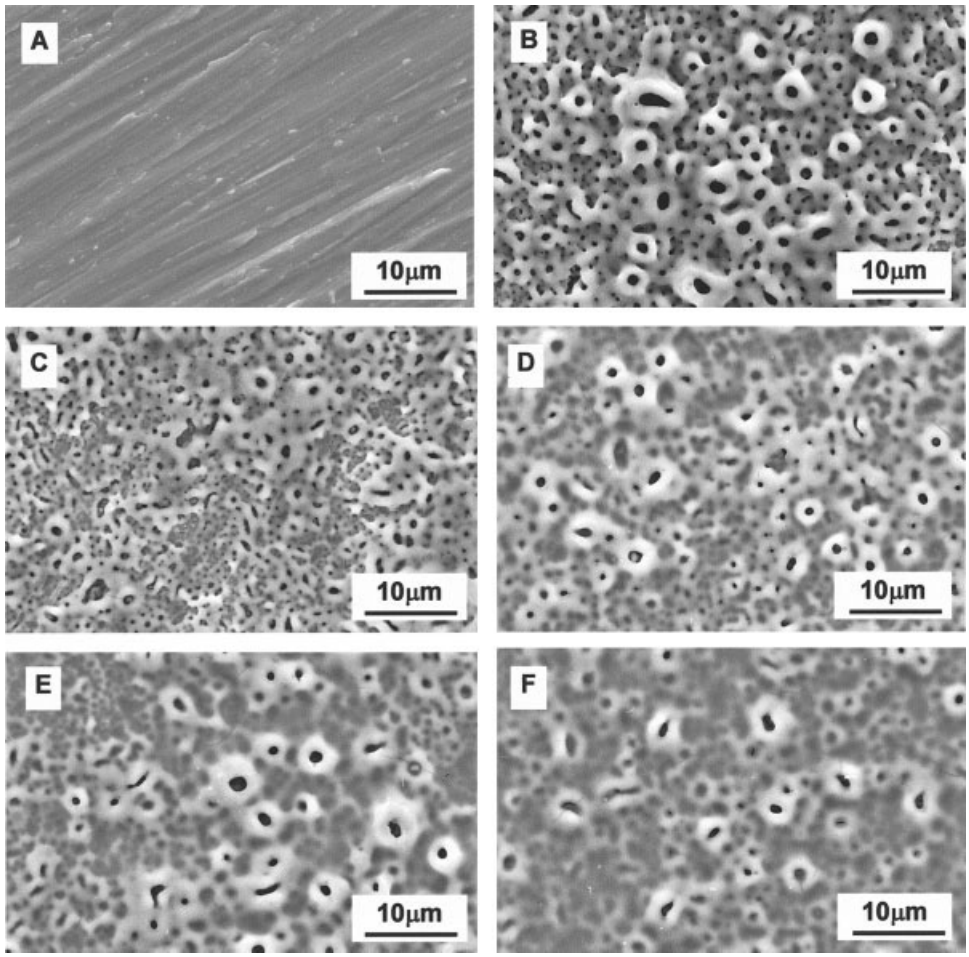

Figure 1. SEM morphologies of (A) pure Ti, (B) MAO-Ti, and HA sol–gel coating on MAO-Ti with sol concentration of (C) 1.5*M*, (D) 2*M*, (E) 3*M*, and (F) 4*M*.

pores became closed, whereas the large pores remained uncovered [Fig. 1(D–F)].

The surface roughness was measured by using a confocal laser scanning microscope, as shown in Figure 2. The average roughness of the MAO-Ti increased significantly ($p < 0.001$), compared with that of pure Ti. With the HA sol–gel coating on the MAO-Ti, the roughness decreased slightly at high concentrations (>2*M*). A statistical difference with respect to the MAO-Ti was observed only for the HA coating deposited with 3*M* sol ($p < 0.05$).

The polished cross-sectional views of the HA sol–gel coating on the MAO-Ti are shown in Figure 3. With MAO treatment at 270 V, a rough oxide layer (2- to 3-μm thickness) was formed on the Ti [Fig. 3(A)]. When the MAO-Ti was coated with 1.5*M* HA sol, a very thin film (100–200 nm) was formed [Fig. 3(B)]. With HA coating at the highest sol concentration (4*M*), a much thicker layer (1–1.5 μm) was formed [Fig. 3(C)]. The formation of the HA outer and TiO_2 inner layers, observed in Figure 3(C), was confirmed by EDS composition analysis, as shown in Figure 3(D). Large amounts of Ca and P were detected in the outer (Ca-P) layer, whereas Ti was dominant in the inner layer. The detection of Ti in the HA layer was due to the interaction volume of the electron beam, and the detection

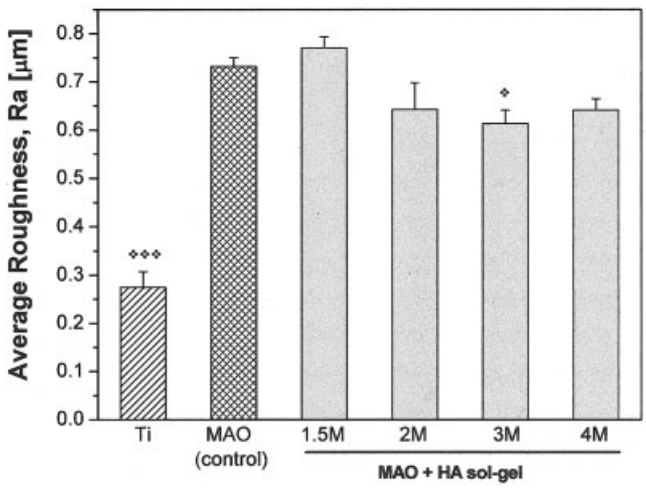

Figure 2. Average roughness of the samples: (❖) $p < 0.05$, (❖❖❖) $p < 0.001$ compared to MAO-Ti.

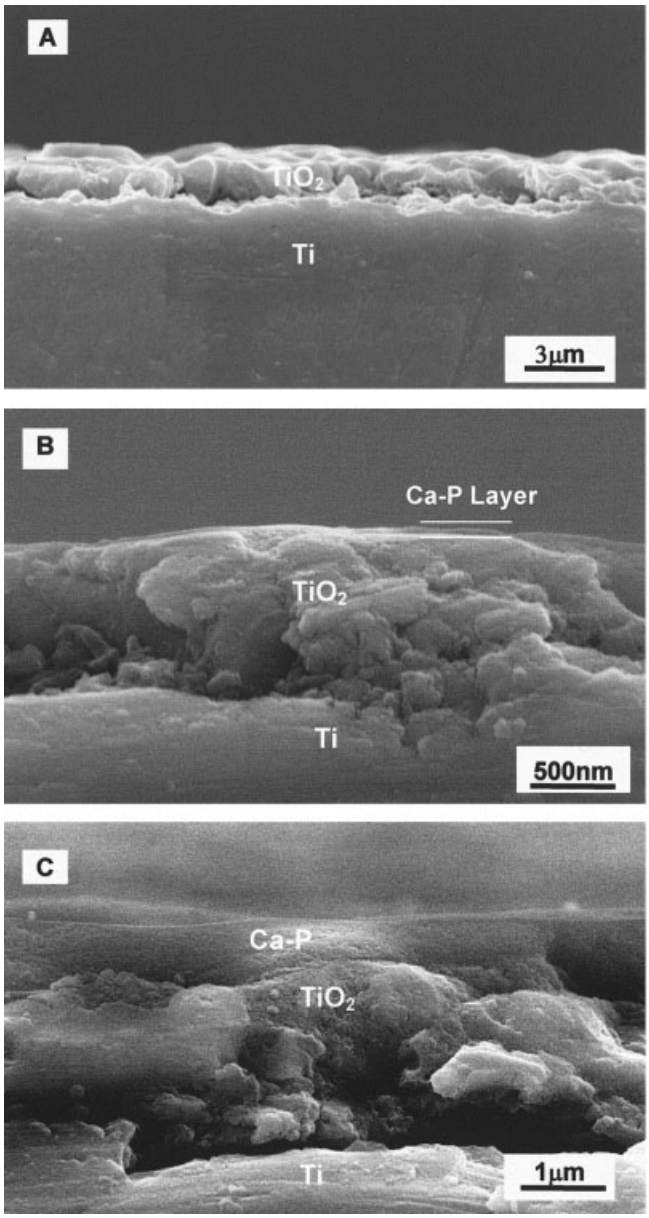

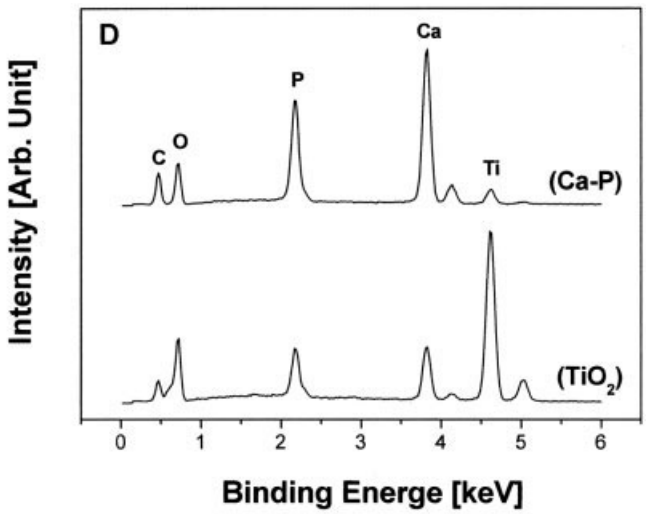

Figure 3. SEM cross-sectional views of (A) MAO-Ti and HA sol–gel coating on MAO-Ti with sol concentration of (B) 1.5*M* and (C) 4*M*. (D) EDS spectra of sol–gel coating and TiO_2 layer of (C).

of Ca and P in the TiO_2 layer resulted from the interaction volume and the incorporation of Ca and P, which occurred because of the MAO treatment.

Coating composition

The atomic composition of the whole coating surface was analyzed by EDS, as shown in Figure 4. On the MAO-Ti surface, the concentrations of Ca and P in the layer were 3.1 and 4.1 at %, respectively. When the HA sol was coated on the MAO-Ti, both the Ca and P concentrations increased. This increase was proportional to the sol concentration. When the sol concentration was 4*M*, the Ca and P concentrations were as high as 9.8 and 7.9 at %, respectively. The concentration of oxygen increased slightly, whereas that of Ti decreased considerably with increasing sol concentration.

The phase of the HA-coated MAO-Ti was analyzed by XRD, as shown in Figure 5. After MAO at 270 V on pure Ti [Fig. 5(A)], a TiO_2 phase (anatase) was formed [Fig. 5(B)]. When the HA sol was coated on the MAO-Ti, an HA phase was observed, and the amount of HA increased with increasing sol concentration [Fig. 5(C–F)].

Cell responses

The SEM morphologies of the HOS cells, which proliferated on the specimens during culturing for 3 days, are shown in Figure 6. On the pure Ti, the cells

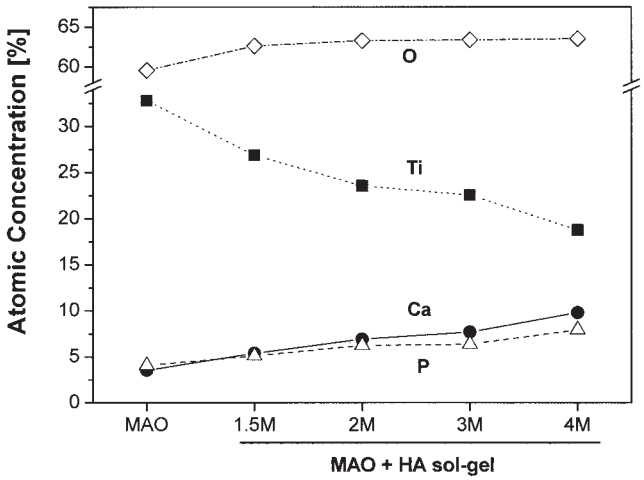

Figure 4. XRD patterns of (A) pure Ti, (B) MAO-Ti, and HA sol–gel coating on MAO-Ti with sol concentration of (C) 1.5*M*, (D) 2*M*, (E) 3*M*, and (F) 4*M*: (■)Ti, (♦) TiO_2 anatase, (❖) Hydroxyapatite.

spread out in an intimate contact with the specimen surface [Fig. 6(A)]. The cells on the MAO-Ti appeared to show slightly less extended cell membranes [Fig. 6(B)]. On the HA-coated surface, on the other hand, the cells spread out more actively [Fig. 6(C,D)].

After 5 days' incubation, the cells proliferated on the specimens were counted, as shown in Figure 7. The number of cells on the HA sol–gel coating on MAO-Ti was significantly higher ($p < 0.001$) than that on the MAO-Ti without the sol–gel coating and increased with increasing sol concentration.

The alkaline phosphatase (ALP) activity of the cells behaved in a similar manner to the proliferation behavior for both culture periods, as shown in Figure 8. The ALP activity of the MAO-Ti was significantly higher ($p < 0.01$) than that of the pure Ti at day 5. When the HA was coated on the MAO-Ti, the ALP level increased significantly compared with the MAO-Ti at both 5 and 10 days. The ALP value increased with increasing sol concentration for both periods.

DISCUSSION

In this report, the biocompatibility of microarc oxidized Ti (MAO-Ti) was found to be further improved by the presence of a sol–gel HA coating. The MAO process is a cost-effective and simple method of producing a porous TiO_2 layer on a Ti implant. Through the MAO treatment, the Ti surface was tailored both physically and chemically to provide beneficial surroundings for the cell ingrowth and bone-bonding ability. Previously, the authors observed that the *in vivo* removal torque of a Ti implant was considerably increased (by a factor of ~3) by MAO treatment at 270 V.[8] Other researchers have also reported enhanced osseointegration on MAO-treated Ti *in vivo*.[4–7] This was mainly attributed to the formation of a biologically favorable phase (TiO_2) and to the morphological changes (porous and rough surface). More importantly, the incorporation of Ca and P from the electrolyte significantly enhanced the biocompatibility of the implant.[4,5,8]

In this respect, the authors attempted to reap the benefits of both the microarc-oxidized morphology and the Ca-P incorporation. First, the Ti was microarc oxidized at 270 V to obtain the benefits associated with the morphological changes, for which the applied voltage was determined on the basis of the highest *in vivo* removal torque observed in our previous study. Subsequently, a thin HA layer was coated on the MAO-Ti using the sol–gel method, because the sol–gel layer is expected to retain the original surface morphology induced by the MAO.

With use of the sol–gel treatment, an HA layer was efficiently deposited on the porous TiO_2 layer. A thin and uniform HA layer was formed throughout the surface. In particular, the roughness was altered very little by the sol–gel treatment, whereas the HA outer layer caused the Ca and P concentrations of the system to be much higher.

The beneficial effects of the HA postcoating were reflected in the *in vitro* cellular responses. The proliferation and ALP activity of the cells were significantly improved by the HA sol–gel coating. When considering the similar roughnesses between the HA-treated and -untreated groups, these results are deemed to be due to the compositional effects. With increasing sol concentration, the proliferation and ALP levels increased, but the compositional benefit appeared to

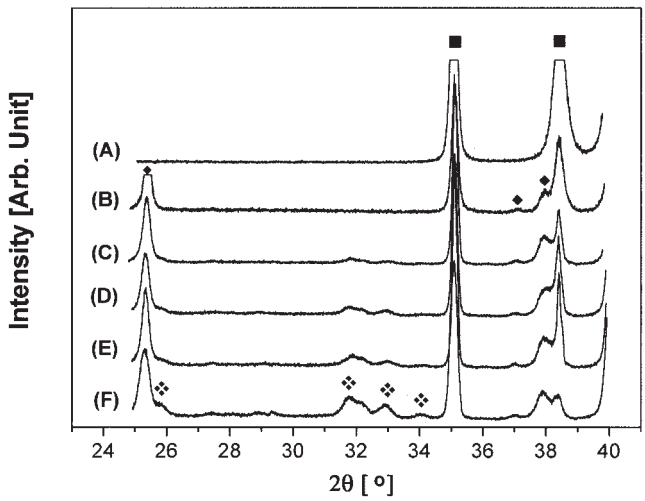

Figure 5. EDS compositional analysis on the surface of the samples.

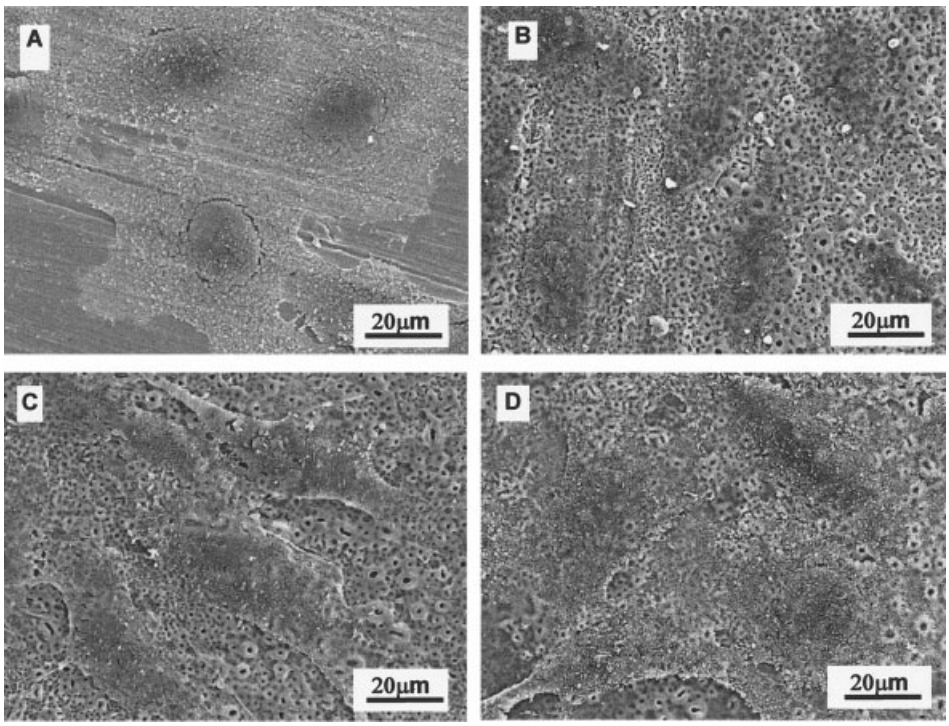

Figure 6. SEM morphology of the HOS cells after culturing for 3 days on (A) pure Ti, (B) MAO-Ti, and HA sol–gel coating on MAO-Ti at sol concentration with (C) 1.5*M* and (D) 3*M*.

reach a peak at a sol concentration of ~3*M*. Because there was little change in surface morphology and roughness up to ~3*M*, this sol concentration is considered to be optimal for enhanced cell responses. These findings on the enhanced cellular responses obtained with the HA posttreatment via the sol–gel method require further confirmation by means of *in vivo* animal tests, before real applications can be envisaged.

CONCLUSIONS

A thin and uniform HA layer was coated on a microarc oxidized Ti (MAO-Ti) substrate by the sol–gel method to improve its biocompatibility. Phase-pure HA was coated, and the coating thickness was controlled by adjusting the sol concentration. With the sol–gel coating, the amounts of Ca and P on the surface increased markedly, whereas the morphology

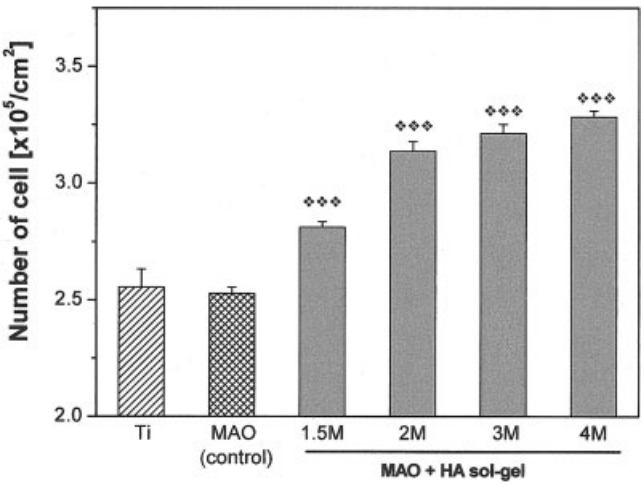

Figure 7. Number of HOS cells proliferated on samples after culturing for 5 days. The error bars represent means ± 1 SD; $n = 6$: (❖❖❖) $p < 0.001$ compared to MAO-Ti.

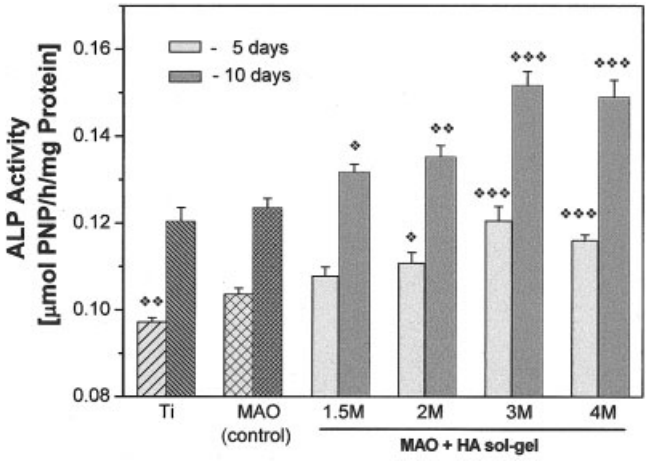

Figure 8. Alkaline phosphatase (ALP) activity of HOS cells cultured for 5 and 10 days. The error bars represent means ± 1 SD; $n = 6$: (❖) $p < 0.05$, (❖❖) $p < 0.01$, and (❖❖❖) $p < 0.001$ compared to MAO-Ti.

and roughness remained unchanged. The sol–gel HA thin layer significantly improved the proliferation and ALP activity of osteoblast-like cells, compared with the MAO-Ti without the HA posttreatment.

References

1. Brunette DM, Tengvall P, Textor M, Thomsen P. Titanium in medicine. Berlin: Springer; 2001.
2. Ishizawa H, Ogino M. Formation and characterization of anodic titanium oxide films containing Ca and P. J Biomed Mater Res 1995;29:65–72.
3. Yerokhin AL, Nie X, Leyland A, Matthews A, Dowey SJ. Plasma electrolysis for surface engineering. Surf Coatings Tech 1999;122:73–93.
4. Sul YT. The significance of the surface properties of oxidized titanium to the bone response: special emphasis on potential biochemical bonding of oxidized titanium implant. Biomaterials 2003;24:3893–3907.
5. Sul YT, Johansson CB, Jeong Y, Röser K, Wennerberg A, Albrektsson T. Oxidized implants and their influence on the bone response. J Mater Sci Mater Med 2001;12:1025–1031.
6. Ishizawa H, Fujino M, Ogino M. Mechanical and histological investigation of hydrothermally treated and untreated anodic titanium oxide films containing Ca and P. J Biomed Mater Res 1995;29:1459–1468.
7. Son WW, Zhu X, Shin HI, Ong JL, Kim KH. *In vivo* histological response to anodized and anodized/hydrothermally treated titanium implants. J Biomed Mater Res Part B Appl Biomater 2003;66B:520–525.
8. Li LH, Kong YM, Kim HW, Kim YW, Kim HE, Heo SJ, Koak JY. Improved biological performance of Ti implants due to surface modification by microarc oxidation. Biomaterials 2004;25:2867–2875.
9. Ishizawa H, Ogino M. Characterization of thin hydroxyapatite layers formed on anodic titanium oxide films containing Ca and P by hydrothermal treatment. J Biomed Mater Res 1995; 29:1071–1079.
10. Kim HW, Koh YH, Li LH, Lee S, Kim HE. Hydroxyapatite coating on titanium substrate with titania buffer layer processed by sol–gel method. Biomaterials 2004;25:2533–2538.
11. Kim HW, Kim HE, Knowles JC. Fluor-hydroxyapatite sol–gel coating on titanium substrate for hard tissue implants. Biomaterials 2004;25:3351–3358.
12. Gan L, Wang J, Tache A, Valiquette N, Deporter D, Pilliar R. Calcium phosphate sol–gel-derived thin films on porous-surfaced implants for enhanced osteoconductivity. Part II. Short-term in vivo studies. Biomaterials 2004;25:5313–5321.
13. Nguyen HQ, Deporter DA, Pilliar RM, Valiquette N, Yakubovich R. The effect of sol–gel-formed calcium phosphate coatings on bone ingrowth and osteoconductivity of porous surfaced Ti alloy implants. Biomaterials 2004;25:865–876.
14. Lacefield WR. Hydroxyapatite coatings. In: Hench LL, Wilson J, editors. An Introduction to Bioceramics. Singapore: World Scientific Publishing Co.; 1993.
15. Hench LL. Bioceramics. J Am Ceram Soc 1998;81:1705–1728.
16. Liu DM, Troczynski T, Tseng WJ. Water-based sol–gel synthesis of hydroxyapatite: process development. Biomaterials 2001; 22:1721–1730.
17. Liu DM, Troczynski T, Tseng WJ. Aging effect on the phase evolution of water-based sol–gel hydroxyapatite. Biomaterials 2002;23:1227–1236.
18. Kim HW, Lee SY, Bae CJ, Noh YJ, Kim HE, Kim HM, Ko JS. Porous ZrO_2 bone scaffold coated with hydroxyapatite with fluorapatite intermediate layer. Biomaterials 2003;24:3277–3284.